# Main Manuscript for

# Low Frequency Oscillations in the Medial Orbitofrontal Cortex Mediate Widespread Hyperalgesia Across Pain Conditions


## Authors

Hyung G. Park[1*], George Kenefati[2, 3], Mika M. Rockholt[2, 3], Xiaomeng Ju[1], Rachel R. Wu[2, 3], Zhen Sage Chen[4, 5, 6], Tamas A. Gonda[7], Jing Wang[2, 3, 5, 6*], Lisa V. Doan[2, 3*]

## Affiliations

[1] Department of Population Health, New York University Grossman School of Medicine, New York, NY, United States
[2] Department of Anesthesiology, Perioperative Care and Pain Medicine, New York University Grossman School of Medicine, New York, NY, United States
[3] Interdisciplinary Pain Research Program, New York University Grossman School of Medicine, New York, NY, United States
[4] Department of Psychiatry, New York University Grossman School of Medicine, New York, NY, United States
[5] Department of Neuroscience & Physiology, New York University Grossman School of Medicine, New York, NY, United States
[6] Department of Biomedical Engineering, New York University Tandon School of Engineering, New York, NY, United States
[7] Department of Medicine, New York University Grossman School of Medicine, New York, NY, United States

*Correspondence:
Hyung G. Park, PhD, hyung.park@nyulangone.org
Jing Wang, MD, PhD, jing.wang2@nyulangone.org
Lisa V. Doan, MD, lisa.doan@nyulagone.org



**Abstract**

Widespread hyperalgesia, characterized by pain sensitivity beyond the primary pain site, is a common yet under-characterized feature across chronic pain conditions, including chronic pancreatitis (CP). In this exploratory study, we identified a candidate neural biosignature of widespread hyperalgesia using high-density electroencephalography (EEG) in patients with chronic low back pain (cLBP). Specifically, stimulus-evoked delta, theta, and alpha oscillatory activity in the bilateral medial orbitofrontal cortex (mOFC) differentiated cLBP patients with widespread hyperalgesia from healthy controls. To examine cross-condition generalizability and advance predictive biomarker development for CP, we applied this mOFC-derived EEG biosignature to an independent cohort of patients with CP. The biosignature distinguished CP patients with widespread hyperalgesia and predicted individual treatment responses to peripherally targeted endoscopic therapy. These preliminary findings provide early support for a shared cortical signature of central sensitization across pain conditions and offer translational potential for developing EEG-based predictive tools for treatment response in CP.



**Keywords:** chronic pancreatitis, chronic pain, widespread hyperalgesia, predictive biomarker, EEG, pain mechanisms

## Introduction

Widespread hyperalgesia is characterized by increased sensitivity to peripheral noxious stimuli in a diffuse, non-anatomic distribution and is considered a marker of impaired central pain processing and nociplastic pain[1-4]. Widespread hyperalgesia can be found in many chronic pain syndromes, including chronic low back pain (cLBP), chronic pancreatitis (CP), fibromyalgia, knee osteoarthritis, and rheumatoid arthritis[5-10]. It is associated with high levels of pain severity and poor response to peripherally-directed treatments[11, 12]. Despite its high prevalence, mechanisms of widespread hyperalgesia remain poorly understood, and while the central nervous system is thought to play a key role, it is unclear if unifying brain mechanisms are shared across multiple pain syndromes.

Neuroimaging studies of the brain have shown structural and functional alterations in chronic pain[13]. Key regions involved in the top-down aversive and cognitive processing of pain include the medial orbitofrontal cortex (mOFC)[10] and prefrontal cortex (PFC)[6, 14]. Recently, intracranial recordings in humans with chronic neuropathic pain showed that spontaneous pain severity was decoded by delta power in the mOFC[14]. Meanwhile, resting state magnetoencephalography recordings in patients with fibromyalgia, a prototypical nociplastic pain condition, also revealed that changes in theta, beta, and gamma power in the mOFC and other prefrontal areas are associated with higher affective pain scores[15].

Advances in source localization has enabled high density (>64 channels) electroencephalogram (EEG) recordings to provide anatomical information to facilitate functional studies[16-18]. For example, amplitudes of beta and gamma oscillations in prefrontal areas were shown to positively correlate with ongoing pain[19, 20]. Abnormal alpha oscillations also play a role in chronic pain[21-23], as the amplitude and timing of peak alpha frequency have been correlated with pain intensity[24-27]. Resting state EEG and functional MRI (fMRI) recordings can provide data regarding chronic alterations in brain circuits in the absence of sensory inputs[28]. Meanwhile, combining highly temporally specific EEG recordings with quantitative sensory testing (QST) that introduces noxious stimuli can assess how the presence of chronic pain alters nociceptive processing[6, 16, 29], to provide insights into mechanisms underlying widespread hyperalgesia[30-33].

In a prior study assessing EEG responses to acute nociceptive stimuli in cLBP participants, we found that altered theta and alpha oscillations in the mOFC and the dorsolateral PFC (dlPFC) were associated with hypersensitivity on QST[6]. A subset of cLBP participants experienced widespread hyperalgesia manifested as hypersensitivity at locations unrelated to the diseased site. However, it is unclear whether stimulus-evoked brain oscillatory activities seen in cLBP patients with widespread hyperalgesia will differ from those seen in patients with localized pain in response to nociceptive input. An even more interesting question is whether specific brain oscillatory findings associated with widespread hyperalgesia in cLBP participants will generalize to widespread hyperalgesia in other chronic pain conditions.

To test whether there are shared brain mechanisms that can function as potential biosignatures for widespread hyperalgesia across different pain conditions, we studied oscillatory activities using high-density (64-ch) EEG recordings during QST at both diseased and disease-free sites in cLBP patients. We focused our inquiry on the mOFC and dlPFC, given their prominent roles in chronic pain phenotypes. We found increased delta and theta oscillations and decreased alpha oscillations in the bilateral mOFC were associated with widespread hyperalgesia in cLBP participants. To test whether these cortical changes reflect a shared mechanism underlying widespread hyperalgesia, we applied this oscillatory brain signature to evoked EEG responses in participants with painful CP. We found that the cLBP-derived EEG signature successfully distinguished widespread hyperalgesia in CP participants. Furthermore, we showed that this biosignature, when evaluated at baseline, successfully predicted pain response in CP patients undergoing endoscopic retrograde pancreatography (ERP) for ductal obstruction, a peripherally-directed treatment that is unlikely to alleviate centrally-mediated pain. These results suggest that

disrupted nociceptive response in the mOFC likely constitutes a common mechanism for widespread hyperalgesia that has the potential to predict treatment responses for chronic pain.

## Results

### A subset of patients in the cLBP and CP cohorts report widespread hyperalgesia

In the cLBP cohort, we recorded stimulus-evoked EEG with mechanical pinprick stimuli of 32 mN and 256 mN to the low back (diseased site) and hand (disease free site). **Table 1** reports baseline participant information for the cLBP cohort and pain-free controls (n=67), including average pain intensity in the prior week, age and sex, stratified by identified pain phenotype: no pain (control), localized pain, and widespread hyperalgesia (see **Methods**)[34]. The participants who experienced pain at an anatomically distant, healthy site (i.e., Widespread Hyperalgesia) comprised about 29% of all the cLBP participants, compatible with previous literature on the incidence of widespread hyperalgesia in chronic pain conditions[1, 3, 4, 35].

Table 1: Chronic low back pain participants show different pain phenotypes (localized pain and widespread hyperalgesia) compared with healthy controls.

| | | No Pain (Control) (n = 25) | Localized Pain (n = 30) | Widespread Hyperalgesia (n = 12) |
|---|---|---|---|---|
| Pain Intensity (mean (SD)) | | 0.28 (0.84) | 5.53 (2.03) | 6.25 (2.38) |
| Age (mean (SD)) | | 46.00 (14.98) | 50.73 (17.18) | 54.25 (14.92) |
| Sex (%) | Female | 5 (20.0%) | 14 (46.7%) | 3 (25.0%) |
| | Male | 20 (80.0%) | 16 (53.3%) | 9 (75.0%) |

**Table 2** reports baseline participant information for the CP cohort (n=18), including age, sex and pain intensity (Brief Pain Inventory-short form (BPI) pain severity subscale, averaged across the four items: Pain Worst, Pain Average, Pain Least, Pain Now), stratified by pain phenotype derived from a standardized pancreatic-specific QST (P-QST) protocol (see **Methods**)[8, 36]. Twelve out of 18 patients were identified as having hyperalgesia, including 8 with widespread hyperalgesia and 4 with localized (i.e., segmental) hyperalgesia.

Table 2: Chronic pancreatitis patients show different pain phenotypes.

| | | No Hyperalgesia (n = 6) | Segmental Hyperalgesia (n = 4) | Widespread Hyperalgesia (n = 8) |
|---|---|---|---|---|
| BPI baseline (mean (SD)) | | 4.29 (2.58) | 3.38 (2.26) | 3.84 (1.41) |
| Age (mean (SD)) | | 61.83 (17.37) | 53.25 (7.37) | 52.50 (17.55) |
| Sex (%) | Female | 0 (0.0) | 2 (50.0) | 4 (50.0) |
| | Male | 6 (100.0) | 2 (50.0) | 4 (50.0) |

### Low-frequency oscillatory changes in the mOFC are associated with widespread hyperalgesia in cLBP participants

We focused our inquiry on the mOFC and dlPFC regions given their roles in chronic pain[6, 10, 14]. After source localization, time- and frequency-resolved oscillatory activity in the mOFC and dlPFC was extracted and analyzed (**Supplementary Figure S1**). To probe nociceptive processing, we applied two different, weighted stimuli (32 mN, non-noxious, and 256 mN, noxious) to back (the site of disease in cLBP participants) and hand (disease-free site). **Supplementary Figure S2** shows time-frequency representations (TFRs) for each pain phenotype group, averaged across participants for the left and right mOFC.

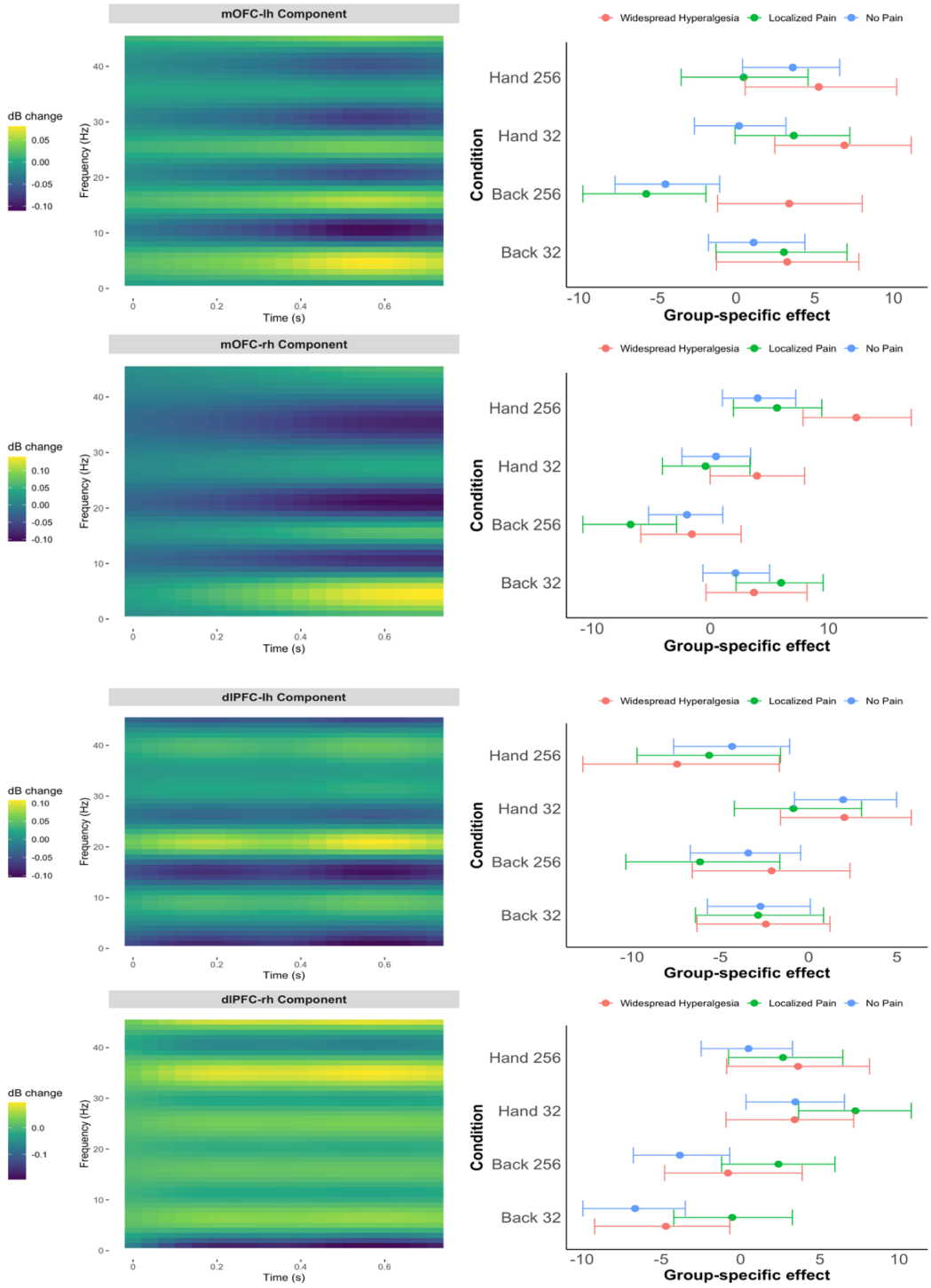


**Figure 1**. **Pain phenotype effects on time-frequency responses in the mOFC (top two rows) and dlPFC (bottom two rows) based on cLBP data (n=67).** Left panels display the data-driven time-frequency basis for the power; right panels show posterior summaries of group-by-condition effects projected onto that basis (means and 90% credible intervals), adjusted for pain intensity, age, and sex. Results are shown by stimulus condition (Back 32 mN, Back 256 mN, Hand 32 mN, Hand 256 mN) and laterality (top row: left hemisphere; bottom row: right hemisphere).

Using multivariate mixed effects models, we modeled how pain phenotype groups (widespread hyperalgesia, localized pain, no pain) influenced EEG time-frequency responses to noxious stimulation in the mOFC and dlPFC, adjusting for age, sex, and pain intensity (**Figure 1**). In the left mOFC (**Figure 1**, first row), the estimated 2D basis for the oscillatory power in the time-frequency domain (left panel) exhibited a characteristic pattern approximately in the 0.4-0.7 second post-stimulus window, with relatively elevated power in the delta/theta (1-7 Hz) range and suppressed power in the alpha (8-12 Hz) range. In this basis, participants with widespread hyperalgesia showed significantly greater stimulus-evoked power than those with localized pain under high-intensity stimulation at the affected site (Back 256 mN), with an estimated group difference of 9.09 (95% CI: [5.61, 12.69]) (**Figure 1**, top row, right panel) (this coefficient, when multiplied by the basis in the left panel, represents the group difference in the time-frequency domain in oscillatory power, expressed in decibels); the corresponding group-level estimates were 3.36 ([–2.08, 9.07]) for widespread hyperalgesia and –5.72 ([–10.73, –1.45]) for localized pain. Similar data-driven time-frequency basis patterns were observed in the right mOFC (**Figure 1**, second row, left panel). However, no statistically significant phenotype group differences were observed in both the left and right dlPFC (**Figure 1**, third and fourth rows).

**Development of an EEG biosignature for widespread hyperalgesia**

The observed differences in low-frequency (delta, theta and alpha) oscillatory activity of the mOFC between participants with widespread versus localized pain a candidate biosignature for widespread hyperalgesia. We defined an EEG-based biosignature as a projection score that quantifies the expression of this characteristic mOFC oscillatory pattern. Specifically, the biosignature was constructed as a weighted sum of the oscillatory power in the left and right mOFC during the 0.4–0.7 second post-stimulus window, under high-intensity stimulation at both affected and unaffected sites and low intensity stimulation at unaffected site. The power in the 1–7 Hz (delta/theta) range was assigned a weight of +1, and the power in the 8–12 Hz (alpha) range was assigned a weight of -1, such that higher scores reflect stronger expression of the widespread hyperalgesia signature—characterized by increased delta/theta and suppressed alpha activity. This time-frequency projection pattern is illustrated in **Figure 2**.

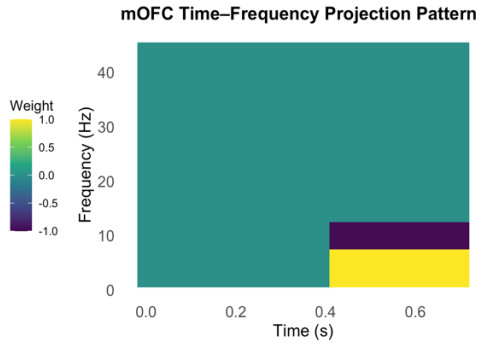


**Figure 2. Time-frequency projection pattern for the mOFC used in biosignature computation.** The pattern highlights increased delta/theta (1–7 Hz) and decreased alpha (8–12 Hz) power during the 0.4–0.7 second post-stimulus window. This weighting scheme was applied to each participant's mOFC time-frequency response (left and right hemispheres, averaged) to compute a scalar biosignature score reflecting expression of the widespread hyperalgesia profile.

**Testing the biosignature for widespread hyperalgesia in a new chronic pain (CP) cohort**

Analogous to the cLBP cohort, in the CP cohort, we applied two levels of mechanical stimulation (32 mN, non-noxious; 512 mN, noxious) to both the upper abdomen (disease-affected site in CP participants) and the forearm (disease-free site). **Supplementary Figure S3** presents group-

averaged time-frequency EEG responses for the CP cohort, stratified by pain phenotype (Widespread, Segmental, No Hyperalgesia). The widespread hyperalgesia group exhibited greater delta/theta (1-7 Hz) power under high-intensity stimulation at the affected site (Abdomen 512 mN) compared to the segmental hyperalgesia group. In contrast, the segmental hyperalgesia group showed relatively reduced delta/theta activity at the unaffected site (Forearm 512 mN) compared to the widespread hyperalgesia group.

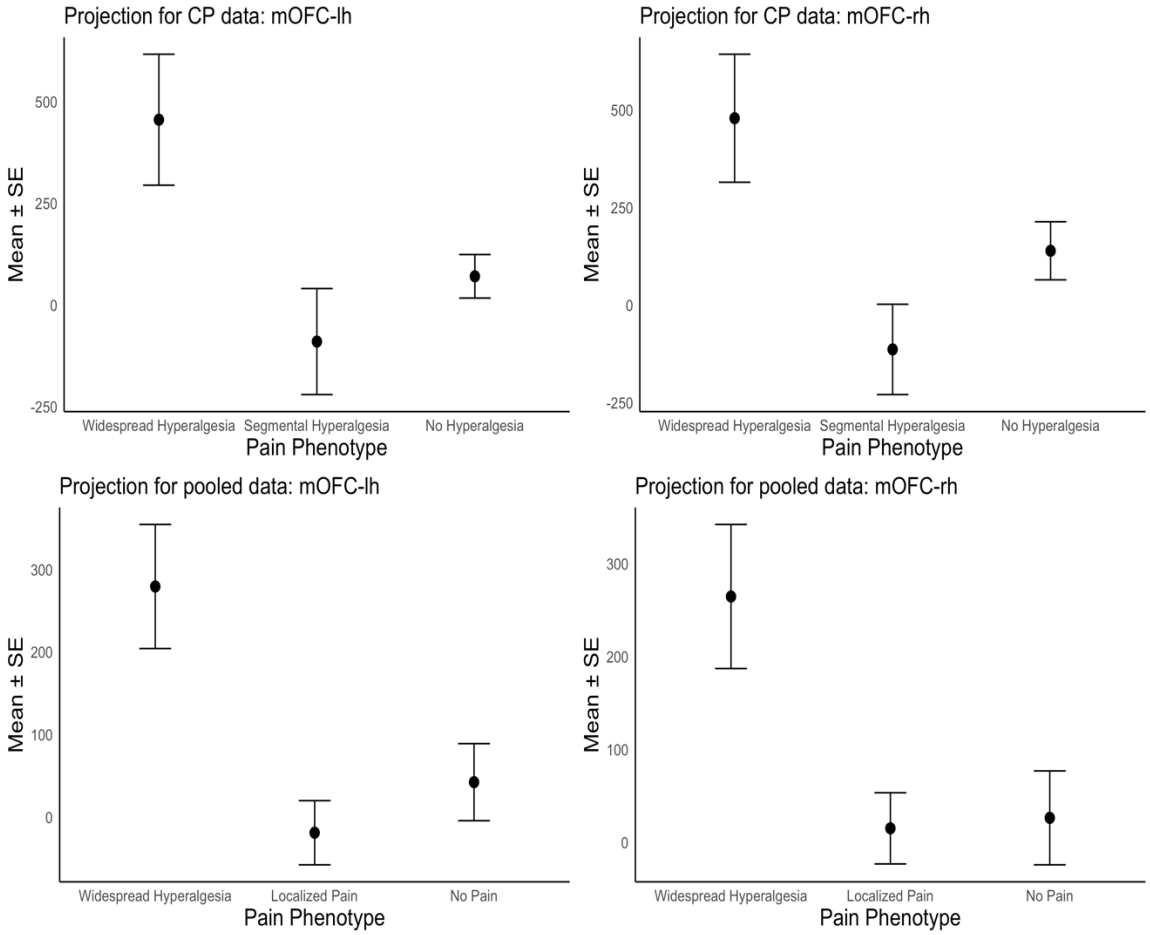


**Figure 3**. **Projection scores onto EEG-based biosignature for widespread hyperalgesia. Top**: **Projection scores onto EEG-based biosignature for widespread hyperalgesia in the CP sample (n=18)**, for the left and right mOFC (left and right panels, respectively). Group means ± standard error of the mean (SEM) are shown for CP participants, stratified by pain phenotype (Widespread, Segmental, No Hyperalgesia), based on projection scores onto the cLBP-derived mOFC biosignature. Projection scores successfully differentiated pain phenotypes based on P-QST classification, with consistent patterns observed across hemispheres.
**Bottom**: **Projection scores onto EEG-based biosignature for widespread hyperalgesia based on the pooled sample (n=85)**, for the left and right mOFC (left and right panels, respectively. Group means ± standard error of the mean (SEM) for participants in the pooled sample, stratified by pain phenotype (Widespread Hyperalgesia, Localized Pain, No Pain), based on projection scores onto the cLBP-derived mOFC biosignature. Projection scores successfully distinguished pain phenotypes based on QST classification, with consistent patterns observed across hemispheres.

To assess the generalizability of mOFC oscillatory features as a marker of widespread hyperalgesia, we applied the cLBP-derived EEG biosignature to participants with CP. **Figure 3** (top panels) displays the mean (± standard error of the mean; SEM) projection scores onto the EEG biosignature for the CP cohort (n = 18), stratified by pain phenotype. Projection of the CP participants' EEG responses onto the biosignature differentiated the three CP pain phenotypes, with comparable discriminative capacity for scores derived from both the left and right mOFC (**Figure 3**, left and right panels, respectively). One-way analysis of variance (ANOVA) indicated statistically significant group differences (left: $p = 0.037$; right: $p = 0.036$) in the CP cohort. Tukey's honest significant difference (HSD) post-hoc comparisons indicated higher projection scores in the widespread hyperalgesia group compared to the segmental hyperalgesia group (left: $p = 0.048$; right: $p = 0.036$). These findings support the cross-condition utility of the cLBP-derived biosignature for detecting widespread hyperalgesia in CP, suggesting that low-frequency oscillatory changes in the mOFC may reflect a shared neurophysiological mechanism.

To further assess the robustness of the signature of widespread hyperalgesia, we pooled data from both the cLBP (n=67) and CP (n=18) cohorts (total n = 85) and repeated the analyses conducted above. We harmonized stimulus conditions across the two chronic pain cohorts for comparability: the affected site was defined as the low back for cLBP and the upper abdomen for CP, while the unaffected site was the hand or forearm in both groups. For this pooled analysis, the "Localized Pain" group included participants with regional pain and either localized hypersensitivity (Segmental Hyperalgesia in CP) or no measurable hyperalgesia (No Hyperalgesia in CP or Localized Pain in cLBP). Consistent with findings from the CP cohort alone, projection of participants' EEG responses onto the biosignature distinguished among the three pain phenotype groups, with similar discriminative capacity for scores derived from the left and right mOFC (**Figure 3**, bottom panels). In the pooled dataset, one-way ANOVA confirmed significant group differences (left: $p < 0.001$; right: $p = 0.003$; **Figure 3**, bottom panels), and Tukey's HSD post-hoc comparisons indicated significantly higher projection scores for the Widespread Hyperalgesia group compared to the Localized Pain group (left: $p < 0.001$; right: $p = 0.004$).

Further, we repeated the analysis presented in **Figure 1**, using the pooled data (n = 85), adjusting for pain intensity, age, sex, and cohort. As in **Figure 1**, **Figure 4** displays the estimated time-frequency basis of the oscillatory power (left panels) alongside posterior summaries of group-by-condition effects projected onto that basis (right panels). Consistent with the cLBP-only analysis, the pooled data revealed a prominent oscillatory pattern in the mOFC—characterized by elevated delta/theta (1–7 Hz) and reduced alpha (8–12 Hz) activity approximately in the 0.4–0.7 second post-stimulus window (**Figure 4**, top left panels)— that differentiated widespread hyperalgesia from localized pain (**Figure 4**, top right panels). These findings reinforce the specificity of the mOFC signature and support its transdiagnostic relevance.

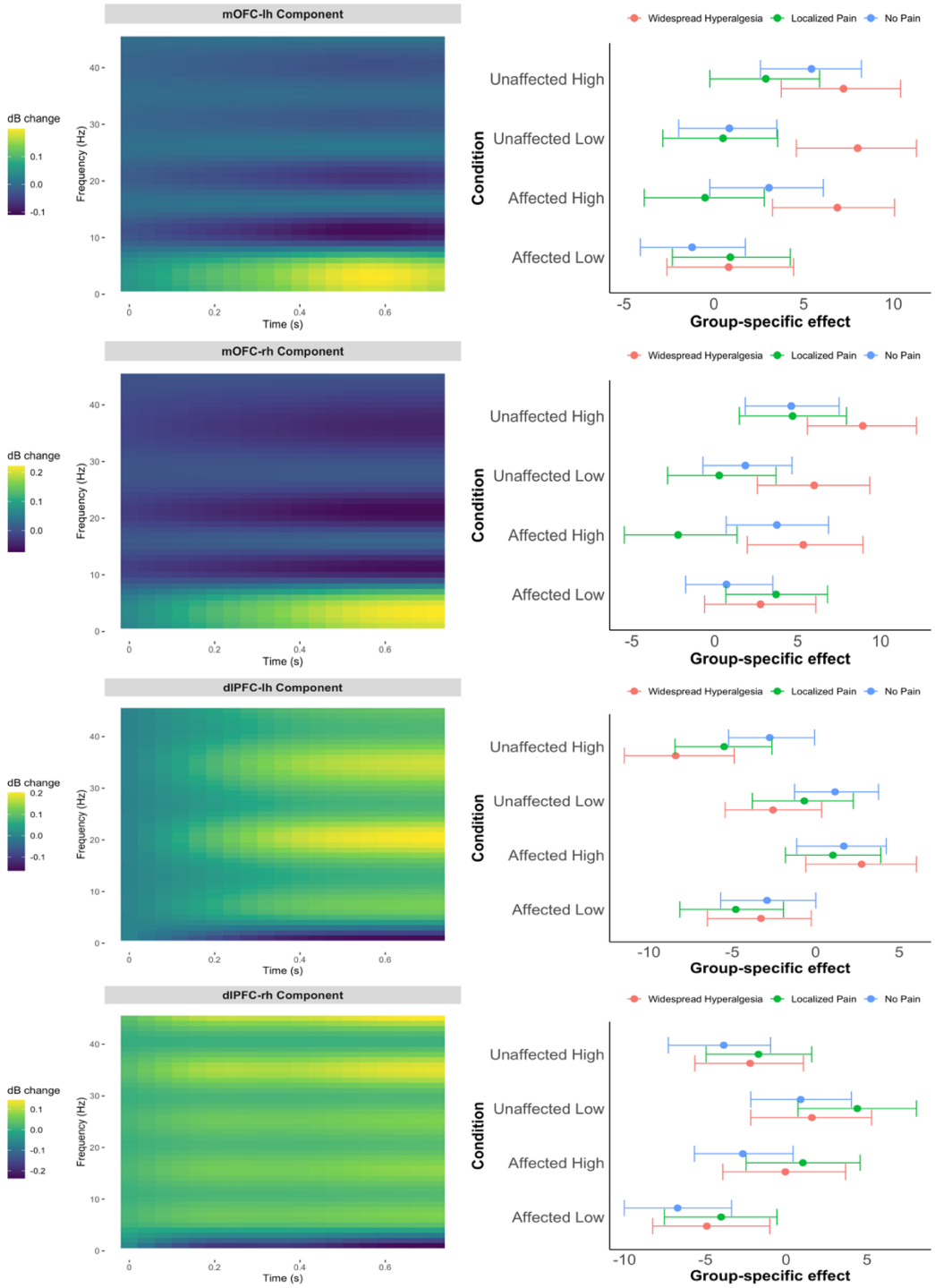


**Figure 4. Pain phenotype effects on time-frequency responses in the mOFC and dlPFC based on pooled data (cLBP and CP; n=85).** Left panels display the data-driven time-frequency basis; right panels show posterior summaries of group-by-condition effects projected onto that basis (means and 90% credible intervals), adjusted for pain intensity, age, sex and cohort. Results are shown by stimulus condition (Affected/Unaffected site and High/Low intensity) and laterality (top: left hemisphere; bottom: right hemisphere). In the pooled analysis, Localized Pain refers to regional pain with either localized hypersensitivity or no measurable hyperalgesia.

**Prediction of treatment response in CP**

A subset of participants in the CP cohort underwent ERP for the treatment of pancreatic ductal obstruction (*n* = 11). ERP is known as a treatment that specifically targets the peripheral mechanisms of pain, but it is thought to have limited efficacy for widespread hyperalgesia that may have central mechanisms, as has been shown for peripherally targeted interventions in other pain conditions associated with widespread hyperalgesia[12, 37]. We assessed pain at 3-months after a technically successful ERP treatment. Among participants without widespread hyperalgesia (n=6), 3 were classified as treatment responders (characterized as ≥30% reduction in BPI pain severity at 3-months relative to baseline BPI, see **Methods**) (**Figure 5**, left panel). In contrast, no responders were observed among those with widespread hyperalgesia (n=5).

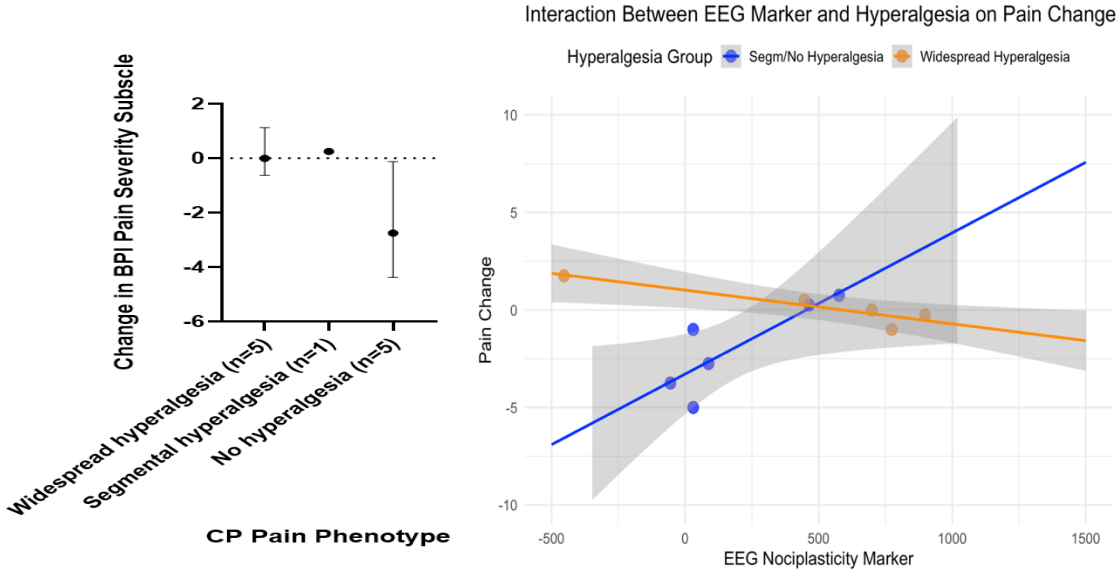


**Figure 5. Pain change stratified by pain phenotypes and EEG biomarker.**
**Left**: **Change in Brief Pain Inventory (BPI) pain severity subscale at 3 months after a technically successful ERP, stratified by pain phenotypes**. Negative values indicate improvement in pain. Values are median and interquartile range (IQR). Overall, participants with widespread or segmental hyperalgesia showed minimal or no responses while participants with no hyperalgesia exhibited better responses, albeit with greater variability.
**Right**: **Scatter plot of baseline EEG biomarker scores versus post-treatment pain change** (negative values indicate pain improvement). Linear regression lines are shown for participants with and without widespread hyperalgesia. The interaction model (EEG × widespread hyperalgesia) that incorporated the EEG marker outperformed models based on the widespread hyperalgesia indicator alone or the 3-level pain phenotypes ($R^2_{adjusted}$= 71% vs. 21% and 27%) and achieved LOOCV AUC = 88% (vs. 63% and 71%).

We next fit a linear regression model using the EEG biosignature, P-QST-derived hyperalgesia phenotype (widespread hyperalgesia vs. segmental or no hyperalgesia), and their interaction to predict 3-month treatment response in CP participants (**Figure 5**, right panel). We compared this multimodal model based on both the EEG biosignature and P-QST-derived phenotype, against two other models for predicting treatment response in CP that are based solely on P-QST results.

Our model that incorporated the EEG biosignature ($R^2$ = 80%; $R^2_{adjusted}$= 71%) substantially outperform these two behavior-based models in terms of the (adjusted) $R^2$: one using only P-QST-based binary widespread hyperalgesia phenotype ($R^2$ = 29%; $R^2_{adjusted}$ = 21%), and another using P-QST-based three-level phenotype (widespread, segmental, and no hyperalgesia) categories ($R^2$ = 42%; $R^2_{adjusted}$= 27%). Among participants without widespread hyperalgesia (i.e., the Segmental/No hyperalgesia group in **Figure 5**, right panel), lower EEG biosignature scores were correlated with improvement in pain, suggesting that combining the mOFC-based biomarker with standard P-QST results can refine phenotyping and produce better prediction for the success of peripherally driven therapies.

Leave-one-out cross-validation (LOOCV) further supported the added predictive value of the EEG biosignature. The interaction model that incorporated the EEG biosignature achieved a LOOCV AUC exceeding 85% (AUC = 88%; accuracy = 82%; sensitivity = 67%; specificity=88%), outperforming the widespread hyperalgesia-only model (LOOCV AUC = 63%; accuracy = 64%; sensitivity = 67%; specificity=63%) and the 3-level categorical phenotype model (LOOCV AUC = 71%; accuracy = 70%; sensitivity = 67%; specificity=71%).

Together, these results indicate that a shared oscillatory brain signature of widespread hyperalgesia may exist across chronic pain conditions (cLBP and CP), and that these cortical nociceptive responses can be leveraged as a biosignature for risk stratification and prediction of treatment response.

## Discussion

In this study, we found that cLBP participants with widespread hyperalgesia, compared to localized or no pain, exhibited a characteristic pattern of increased delta/theta coupled with decreased alpha oscillatory power in the mOFC during noxious pinprick stimulation. Based on these findings, we derived a biosignature of widespread hyperalgesia and found that this cLBP-derived marker can be effectively applied to CP participants, a distinct chronic patient population, for pain phenotype differentiation. Notably, CP participants with more widespread hyperalgesia, compared to segmental or no hyperalgesia, showed an elevated expression of the mOFC delta–theta oscillatory marker with alpha suppression. Despite differences in peripheral pathology between cLBP and CP, our results suggest a potential common central mechanism for widespread hyperalgesia.

### Role for mOFC in widespread hyperalgesia

The involvement of mOFC in widespread hyperalgesia is compatible with its role in affective and cognitive pain modulation. This region is known to receive signals from and in turn project to multiple cortical areas. The oscillatory changes observed in mOFC may thus reflect reduced cortical inhibition (increased oscillatory power in slow-wave bands), consistent with prior literature[26, 27, 33]. For example, increased theta activity has been reported in participants with various chronic pain conditions, both in resting state recordings as well as evoked EEG potentials[28, 38-43]. In our cLBP cohort, painful stimulation at the site of injury (lower back) evoked significantly greater theta-band responses, with a relative alpha suppression, in participants with widespread hyperalgesia compared to localized pain or pain-free controls. Compatible with our findings here, a recent study in chronic pain participants with chronic intracranial recordings showed that changes in oscillatory activities in the OFC can function as a biomarker for chronic pain[14]. Other studies have shown that mOFC has prominent roles in reward processing as well as placebo analgesia[44, 45].

Placing our specific findings on nociceptive processing in widespread hyperalgesia within the current literature, a model emerges in which the mOFC acts as a critical hub in central regulation of pain, by integrating cognitive-affective information with sensory-nociceptive signals. As a result,

when the activity of mOFC is dysregulated, there is decreased top-down regulation, resulting in widespread hyperalgesia and pain amplification.

**Mechanism-based biosignature for widespread hyperalgesia**

Methodologically, we leveraged projection-based biomarker construction to develop an EEG index of widespread hyperalgesia. To assess generalizability, we projected CP participants' EEG responses onto the cLBP-derived oscillatory signature. This cross-condition application suggests the promise of EEG-derived markers in identifying central pain amplification. Rather than relying on a single frequency band, our biosignature incorporates the multi-band oscillatory pattern (delta/theta increase with alpha decrease in mOFC) as a composite feature. We achieved this by identifying the mOFC time-frequency representation (TFR) that best differentiated the widespread hyperalgesia subgroup and then projecting individual EEG data onto this signature to yield a scalar index for each participant, that can be compared across individuals.

In both the cLBP and CP cohorts, biomarker values showed a consistent difference between widespread hyperalgesia vs. segmental hyperalgesia or localized pain. Our biosignature, defined as increased delta/theta and decreased alpha power in the mOFC during the 0.4-0.7 second post-stimulus window, appears to reflect the extent of central affective-cognitive engagement in pain processing. Participants with widespread hyperalgesia showed higher biosignature values, consistent with greater centralized sensitization and diminished top-down inhibitory control. In contrast, participants with localized hyperalgesia exhibited lower biosignature values, suggesting a pain phenotype with less mOFC-mediated central component, with pain dominated by peripheral mechanisms. These findings support the utility of mOFC-based oscillatory activities as a marker that represents the spectrum of widespread hyperalgesia.

**Predictive value for an EEG biosignature in chronic pain syndromes**

Our EEG biosignature differentiated pain phenotypes. More importantly, it predicted 3-month treatment outcomes in CP participants, outperforming P-QST-based signatures of widespread hyperalgesia. Higher scores of our biosignature were associated with poor treatment response among participants without hyperalgesia, suggesting its potential for early identification of at-risk individuals and personalization of therapy.

Both cLBP and CP are clinically heterogeneous. In some patients, pain is dominantly driven by ongoing peripheral nociceptive, inflammatory or neuropathic processes, while others develop a disproportionate or widespread pain sensitivity that may have a strong component of central amplification or nociplastic pain. Differentiation between peripherally vs. centrally-driven pain is clinically important, as it can inform treatment selections. Participants who have pronounced central amplification may not respond to therapies targeting peripheral processes. Identifying individuals with CP associated with widespread hyperalgesia will have important impact on their treatment as these individuals would likely not benefit from pancreatic targeted interventions such as ERP or surgery. Prior studies have explored the use of QST to identify participants more likely to benefit from peripheral interventions like ERP, particularly those without central sensitization[46, 47]. Our results here indicate that addition of EEG biosignature to P-QST can enhance the predictive accuracy by further explaining the heterogeneous responses to ERP.

**A transfer learning approach to study mechanisms of chronic pain**

While this study focused on cLBP and CP, the concept of a shared nociplastic EEG signature may extend to other chronic pain conditions involving central sensitization (e.g., migraine, osteoarthritis). Our success to transfer oscillatory signatures that we learned from cLBP to CP highlights potential shared neurophysiological mechanisms of widespread hyperalgesia and underscores the potential use of EEG-based biomarkers for cross-condition phenotyping. This transfer learning approach offers a data-efficient strategy to accelerate biomarker development in underpowered clinical populations.

## Limitations and future directions

Key limitations include the small sample size in the CP cohort (n = 18) precluding reliable estimation of oscillatory effects of widespread hyperalgesia from the CP cohort alone, and the lack of an independent validation dataset for predictive models. Thus, the EEG biosignature derived here should be prospectively tested as a stratification tool at baseline to track clinical outcomes longitudinally in a larger cohort to further validate its predictive accuracy. Longitudinal studies could also assess how the EEG signature changes with effective treatment and whether it can serve as an objective treatment-induced neuroplasticity measure. Furthermore, our analyses focused on local oscillatory power changes in specific brain regions and did not examine functional connectivity or network-level interactions. Incorporating EEG connectivity or graph theoretical metrics in future work could enrich our understanding of how widespread hyperalgesia emerges from distributed brain circuit dysfunction and could yield multi-feature biomarkers that further improve classification accuracy. Another important direction is to integrate EEG with structural and functional neuroimaging to build a more comprehensive biomarker. Structural MRI could be used to see if there are anatomical correlates of the EEG signature (e.g., cortical thinning in those with high mOFC theta power)[48]. Combining EEG and fMRI simultaneously can also leverage the strengths of each modality to more precisely characterize the nociplastic signature[49].

## Summary

We identified an mOFC-based EEG signature of widespread hyperalgesia that may serve as a mechanistic marker of pain amplification across two different chronic pain syndromes. Our results suggest potential shared mechanisms among widespread hyperalgesia and the possibility of mechanistically driven biomarkers that can predict treatment success to advance precision pain medicine.

# Materials and Methods

We analyzed data from 85 pooled sessions of QST and simultaneous high-density EEG recordings, drawn from two prospective cohort studies. Both studies were approved by the NYU Grossman School of Medicine IRB (8/22/2019, #i19-01088; 9/18/2023, #i23-00766) and conducted in accordance with the Declaration of Helsinki. All participants provided written informed consent.

## Study Participants and Eligibility Criteria

Data were collected from two cohorts: 38 cLBP participants (including 4 with long-term longitudinal follow-up; n = 42) vs. 25 pain-free controls, and 18 participants with painful CP. cLBP inclusion criteria included adults aged 18 to75 years with pain lasting greater than 6 months and baseline average pain intensity > 4 on a 0 to10 point numerical rating scale (NRS), with exclusion criteria including acute lumbosacral radiculopathy with motor or sensory loss, systemic symptoms, history of cognitive impairment or clinical signs of altered mental status, history of schizophrenia, daily benzodiazepine use, and pregnancy. Inclusion criteria for pain-free healthy controls included age 18 to 75 years and American Society of Anesthesiologists (ASA) physical status 1-3. CP inclusion criteria included adults older than 18 years with Cambridge III-IV or M-ANNHEIM criteria for definitive chronic pancreatitis[50, 51], pain present ≥ 3 days per week for ≥ 3 months with average pain ≥ 4 on the 0 to 10 point NRS and scheduled for endoscopic therapy for ductal obstruction. Exclusion criteria included recent acute pancreatitis within 2 months of enrollment, technically successful ERP in 3 months prior to enrollment, active illicit drug use (excluding marijuana) or chronic benzodiazepine use, ASA physical status > 3, immune-mediated pancreatitis, pancreatic neoplasms, major neurological disease, and pregnancy. At baseline, pain was assessed in the cLBP cohort with the PROMIS pain intensity 1a questionnaire which

assesses average pain in the prior week. In the CP cohort, pain was assessed with the BPI[52]. The BPI pain severity subscale was used to characterize pain intensity.

**EEG Recordings**

EEG data were recorded using a 64-channel cap (G.Tec or Compumedics Neuroscan) equipped with two integrated bipolar leads for vertical electrooculogram with the ground electrode positioned on the left cheek, sampled at 1000 Hz and filtered between 0.5–100 Hz. Each recording session began with baseline recordings with 5 minutes eyes closed and 5 minutes eyes opened. For each participant, stimulus-evoked EEG was recorded during mechanical pinprick stimuli at four stimulus conditions (see below). See **Figure 6** for the experiment scheme.

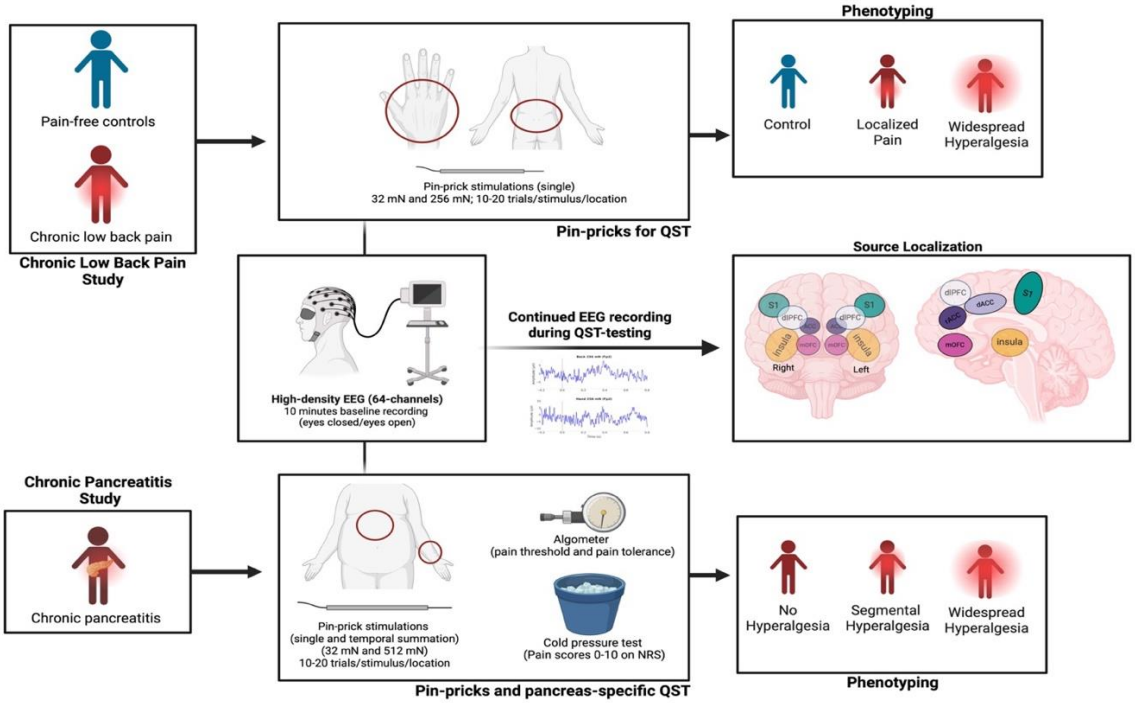


**Figure 6. Schematic overview of the experimental design for concurrent QST and EEG**. **Left panels**: Participants with chronic low back pain (cLBP) and chronic pancreatitis (CP) were enrolled. **Middle panels**: EEG was recorded during pinprick stimulation at the lower back and dorsum of the right hand (for cLBP), and at the upper abdomen and dominant forearm (for CP). **Right panels**: Participants were pain-phenotyped, and EEG source localization was performed, focusing on mOFC and dlPFC as regions of interest (ROIs).

**QST Protocols**

In the cLBP cohort (n = 67), participants (with cLBP and pain-free healthy controls) were blindfolded and instructed to remain relaxed but awake during EEG recordings. Mechanical pinprick stimuli (MRC Systems GmbH, Heidelberg, Germany) were applied to the lower back (pain affected site for cLBP participants) and the dorsum of the right hand (site typically unaffected by pain) using forces of 32 mN and 256 mN. Each force was delivered in 10-20 randomized trials per site with an interstimulus interval of approximately 10 seconds, and participants rated each stimulus on the 0 to 10 point NRS scale.

Analogous to the cLBP cohort, the CP cohort (n=18) underwent a stimulus-evoked EEG protocol. Mechanical pinprick stimuli of 32 mN and 512 mN were applied to the upper abdomen (pain affected site in CP) and the dominant forearm (site typically unaffected by pain in CP). Participants rated each stimulus on the NRS scale. CP participants also underwent a standardized pancreatic QST (P-QST) protocol[8, 36]. Briefly, participants received repetitive pinprick stimulation with a 256 mN force to assess temporal summation at both the upper abdomen and the midline volar forearm of the dominant arm. CP participants underwent muscle pressure testing using an algometer (Algometer Type II, SBMEDIC Electronics, Solna, Sweden) to determine pressure pain detection thresholds (PDT) and pain tolerance thresholds (PTT). Pressure was applied to the following dermatomes: C5 (clavicle), T10 (upper epigastric area—pancreatic viscerotome), T10 back (posterior pancreatic viscerotome), L1 (anterior superior iliac crest), and L4 (quadriceps). Lastly, the conditioned pain modulation (CPM) was assessed with a cold pressor test, in which the dominant hand was immersed in ice-chilled water for up to 120 seconds, and PTT at the non-dominant quadriceps muscle, measured before and after the cold pressor test.

**Pain Phenotyping**

For the cLBP cohort, a threshold for hyperalgesic response to 32 mN stimulation at the hand (a site typically unaffected by pain) was defined as 2 standard deviations above the mean pain rating in control participants[34]. cLBP participants below this threshold were classified as having localized Pain, whereas those above the threshold were classified as having widespread hyperalgesia. Control participants were classified as no pain.

For the CP participants, pain phenotypes were defined using the published algorithm for the P-QST protocol[8, 36] defined based on cold pressor test, CPM, PDT, and temporal summation distinguishing the participants into three groups: no hyperalgesia, segmental hyperalgesia, and widespread hyperalgesia.

**Standardized ERP in CP Cohort and Pain Outcome**

As part of routine standard of care, CP participants underwent standardized ERP. A technically successful procedure was defined as stent placement across a pancreatic duct stricture and/or removal of obstructing stone or intraductal calcification. BPI was assessed at baseline before ERP and at approximately 3 months after a technically successful procedure.

**EEG Preprocessing**

Preprocessing included notch filtering (at 60 Hz with 3 Hz notch width) to remove powerline noise, band-pass filtering, bad channel detection and interpolation using the PyPREP toolbox, and artifact correction via independent component analysis (ICA)[53-55]. Source localization was performed using the MNE-Python toolbox with the minimum norm estimate (MNE) method, employing a boundary-element head model and Desikan-Killiany atlas. Time-frequency representations were computed using the mne.time_frequency.tfr_multitapter function from the MNE-Python toolbox with default parameters[56]. EEG data were epoched from -1 to 1 second relative to stimulus onset for each trial, and spectral decomposition was performed across the 0.5-100 Hz frequency range, excluding 58–61 Hz to suppress residual line noise. The multitaper method provides robust spectral estimates by averaging across multiple orthogonal tapers.

For analysis, epochs were extracted from -0.3 to 0.7 seconds relative to each pinprick stimulus onset. Time-frequency representations (TFRs) of the oscillatory power (1 to 45 Hz) were computed using real and imaginary signal components of the decomposition and transformed into decibel scale[3, 57]. Baseline correction was performed by subtracting the average pre-stimulus power (-0.3 to 0 s) for each trial per frequency. Corrected dB power responses were then averaged across trials to yield subject- and stimulus condition-specific TFRs for each of the four regions of interest (bilateral mOFC and dlPFC). Each resulting TFR was stored as a time (T) × frequency (F) matrix, downsampled to approximately 37 ms resolution (T = 27, F = 45).

**Statistical Modeling for cLBP Cohort**

We modeled baseline-corrected TFRs in the 0 to 0.7 second post-stimulus window as 2D functional outcomes (time × frequency) using a Bayesian mixed-effects framework[58, 59]. For each ROI, we jointly modeled stimulus-evoked responses across four conditions (Back 32 mN, Back 256 mN, Hand 32 mN, Hand 256 mN). The model included fixed effects for group (Widespread, Localized, No Pain), age, sex, and PROMIS pain intensity, and random intercepts for subjects, as well as subject-by-condition random effects, to account for within-subject residual correlation. To represent 2D TFR responses, we used a bivariate cubic B-spline basis (5 × 10 dimensions for time and frequency). Fixed effects were projected onto a rank-1 representation using an automatic rank selection procedure. Covariate coefficients were given zero-mean normal priors with hierarchical shrinkage priors on their variances. The fixed effects' basis was modeled as an outer product of unit-norm time and frequency vectors with uniform priors on the unit sphere. Random effect coefficients received independent zero-mean normal priors with Inverse-Gamma hyperpriors on variances. Measurement error variances had Jeffreys' priors. We used 1500 burn-in and 500 post-burn-in MCMC iterations. All EEG preprocessing and modeling steps were conducted using MNE-Python, R (including rhdf5 and ggplot2), and custom analysis pipelines developed for this project.

**Transfer Learning for CP Cohort in Predicting Treatment Response**

The limited sample size of the CP cohort (n = 18) constrained our ability to directly infer reliable signatures of widespread hyperalgesia within the CP group alone. To address this, we first modeled TFR responses in the cLBP cohort (n = 67) to identify frontal cortical signatures (mOFC and dlPFC) associated with widespread hyperalgesia. This group-level effect analysis in the cLBP cohort informed the development of an EEG-based biomarker of widespread hyperalgesia, which was then applied to the CP cohort to assess its generalizability and predictive value. Specifically, we projected each CP participant's TFR responses onto the cLBP-derived oscillatory signatures and examined whether these projections distinguished pain phenotypes (widespread, segmental, or no hyperalgesia) and predicted treatment (ERP) response in CP. This cross-cohort application in developing predictive models represents a transfer learning framework[60, 61], leveraging statistical features learned in one population (cLBP) to refine pain phenotyping in another (CP) and use these features to help develop clinical prediction models in CP.

Group differences in biosignature projection scores among CP participants were evaluated using one-way ANOVA, followed by Tukey's HSD tests for post-hoc pairwise comparisons. To predict 3-month ERP response in CP participants, we fit a linear regression model using the cLBP-derived mOFC biosignature, the P-QST-derived hyperalgesia phenotype (widespread vs. segmental/no) and their interaction. Model performance was compared to two alternative models based solely on P-QST phenotypes (the widespread hyperalgesia model and the three-group phenotype model), with respect to the (adjusted) $R^2$ and leave-one-out cross-validation (LOOCV) area under the receiver operating characteristic curve (AUC).

**Acknowledgments**

**Funding:** National Institutes of Health grant UG3NS135170 (LVD, ZSC, TAG, HGP, JW)

**Data and materials availability**

All code and processed data used in this study are available at https://github.com/syhyunpark/mOFC-EEG-biosignature-hyperalgesia. The repository includes scripts and data necessary to reproduce all analyses, figures, and tables presented in this preprint. Data from the CP cohort will be deposited in the NIMH Data Archive as part of our funded study.

**Author Contributions:** Conceptualization: HGP, ZSC, TAG, JW, LVD; Methodology: HGP, XJ, TAG, JW, LVD; Investigation: MMR, RRW, TAG, JW, LVD; Visualization: HGP, XJ, MMR, GK, LVD; Supervision: HGP, TAG, JW, LVD; Writing—original draft: HGP, JW, LVD; Writing—review & editing: All

**Competing Interest Statement:** JW is the founder and scientific advisor for Pallas Technologies; the remaining authors have no competing interests to declare.

## References


1. Latremoliere A, Woolf CJ. Central sensitization: a generator of pain hypersensitivity by central neural plasticity. J Pain. 2009;10(9):895-926. doi: 10.1016/j.jpain.2009.06.012. PubMed PMID: 19712899; PMCID: PMC2750819.
2. Kosek E, Cohen M, Baron R, Gebhart GF, Mico JA, Rice ASC, Rief W, Sluka AK. Do we need a third mechanistic descriptor for chronic pain states? Pain. 2016;157(7):1382-6. doi: 10.1097/j.pain.0000000000000507. PubMed PMID: 26835783.
3. Nijs J, George SZ, Clauw DJ, Fernández-de-Las-Peñas C, Kosek E, Ickmans K, Fernández-Carnero J, Polli A, Kapreli E, Huysmans E, Cuesta-Vargas AI, Mani R, Lundberg M, Leysen L, Rice D, Sterling M, Curatolo M. Central sensitisation in chronic pain conditions: latest discoveries and their potential for precision medicine. Lancet Rheumatol. 2021;3(5):e383-e92. Epub 20210330. doi: 10.1016/s2665-9913(21)00032-1. PubMed PMID: 38279393.
4. Fitzcharles MA, Cohen SP, Clauw DJ, Littlejohn G, Usui C, Häuser W. Nociplastic pain: towards an understanding of prevalent pain conditions. Lancet. 2021;397(10289):2098-110. doi: 10.1016/s0140-6736(21)00392-5. PubMed PMID: 34062144.
5. Sluka KA, Clauw DJ. Neurobiology of fibromyalgia and chronic widespread pain. Neuroscience. 2016;338:114-29. Epub 20160609. doi: 10.1016/j.neuroscience.2016.06.006. PubMed PMID: 27291641; PMCID: PMC5083139.
6. Kenefati G, Rockholt MM, Ok D, McCartin M, Zhang Q, Sun G, Maslinski J, Wang A, Chen B, Voigt EP, Chen ZS, Wang J, Doan LV. Changes in alpha, theta, and gamma oscillations in distinct cortical areas are associated with altered acute pain responses in chronic low back pain patients. Front Neurosci. 2023;17:1278183. Epub 20231013. doi: 10.3389/fnins.2023.1278183. PubMed PMID: 37901433; PMCID: PMC10611481.
7. Aoyagi K, He J, Nicol AL, Clauw DJ, Kluding PM, Jernigan S, Sharma NK. A Subgroup of Chronic Low Back Pain Patients With Central Sensitization. Clin J Pain. 2019;35(11):869-79. doi: 10.1097/ajp.0000000000000755. PubMed PMID: 31408011; PMCID: PMC7197191.
8. Faghih M, Phillips AE, Kuhlmann L, Afghani E, Drewes AM, Yadav D, Singh VK, Olesen SS. Pancreatic QST Differentiates Chronic Pancreatitis Patients into Distinct Pain Phenotypes Independent of Psychiatric Comorbidities. Clin Gastroenterol Hepatol. 2022;20(1):153-61.e2. Epub 20201022. doi: 10.1016/j.cgh.2020.10.036. PubMed PMID: 34108130; PMCID: PMC8629107.
9. Neville SJ, Clauw AD, Moser SE, Urquhart AG, Clauw DJ, Brummett CM, Harte SE. Association Between the 2011 Fibromyalgia Survey Criteria and Multisite Pain

Sensitivity in Knee Osteoarthritis. Clin J Pain. 2018;34(10):909-17. doi: 10.1097/ajp.0000000000000619. PubMed PMID: 29642237; PMCID: PMC6110956.
10. Heisler AC, Song J, Dunlop DD, Wohlfahrt A, Bingham CO, III, Bolster MB, Clauw DJ, Marder W, Phillips K, Neogi T, Lee YC. Association of Pain Centralization and Patient-Reported Pain in Active Rheumatoid Arthritis. Arthritis Care Res (Hoboken). 2020;72(8):1122-9. Epub 20200721. doi: 10.1002/acr.23994. PubMed PMID: 31162824; PMCID: PMC6891118.
11. Vigotsky AD, Cong O, Pinto CB, Barroso J, Perez J, Petersen KK, Arendt-Nielsen L, Hardt KD, Manning D, Apkarian AV, Branco P. Prognostic value of preoperative mechanical hyperalgesia and neuropathic pain qualities for postoperative pain after total knee replacement. Eur J Pain. 2024;28(8):1387-401. Epub 20240608. doi: 10.1002/ejp.2295. PubMed PMID: 38850090.
12. Heisler AC, Song J, Muhammad LN, Wohlfahrt A, Marder W, Bolster MB, Bingham CO, 3rd, Clauw DJ, Dunlop DD, Neogi T, Lee YC. Association of Dysregulated Central Pain Processing and Response to Disease-Modifying Antirheumatic Drug Therapy in Rheumatoid Arthritis. Arthritis Rheumatol. 2020;72(12):2017-24. Epub 20201104. doi: 10.1002/art.41440. PubMed PMID: 32683800; PMCID: PMC8078061.
13. Martucci KT, Mackey SC. Neuroimaging of Pain: Human Evidence and Clinical Relevance of Central Nervous System Processes and Modulation. Anesthesiology. 2018;128(6):1241-54. doi: 10.1097/aln.0000000000002137. PubMed PMID: 29494401; PMCID: PMC5953782.
14. Shirvalkar P, Prosky J, Chin G, Ahmadipour P, Sani OG, Desai M, Schmitgen A, Dawes H, Shanechi MM, Starr PA, Chang EF. First-in-human prediction of chronic pain state using intracranial neural biomarkers. Nat Neurosci. 2023;26(6):1090-9. Epub 20230522. doi: 10.1038/s41593-023-01338-z. PubMed PMID: 37217725; PMCID: PMC10330878.
15. Lim M, Kim JS, Kim DJ, Chung CK. Increased Low- and High-Frequency Oscillatory Activity in the Prefrontal Cortex of Fibromyalgia Patients. Front Hum Neurosci. 2016;10:111. Epub 20160314. doi: 10.3389/fnhum.2016.00111. PubMed PMID: 27014041; PMCID: PMC4789463.
16. Rockholt MM, Kenefati G, Doan LV, Chen ZS, Wang J. In search of a composite biomarker for chronic pain by way of EEG and machine learning: where do we currently stand? Front Neurosci. 2023;17:1186418. Epub 20230614. doi: 10.3389/fnins.2023.1186418. PubMed PMID: 37389362; PMCID: PMC10301750.
17. Sun R, Sohrabpour A, Worrell GA, He B. Deep neural networks constrained by neural mass models improve electrophysiological source imaging of spatiotemporal brain dynamics. Proc Natl Acad Sci U S A. 2022;119(31):e2201128119. Epub 20220726. doi: 10.1073/pnas.2201128119. PubMed PMID: 35881787; PMCID: PMC9351497.
18. Seeber M, Cantonas LM, Hoevels M, Sesia T, Visser-Vandewalle V, Michel CM. Subcortical electrophysiological activity is detectable with high-density EEG source imaging. Nat Commun. 2019;10(1):753. Epub 20190214. doi: 10.1038/s41467-019-08725-w. PubMed PMID: 30765707; PMCID: PMC6376013.
19. May ES, Nickel MM, Ta Dinh S, Tiemann L, Heitmann H, Voth I, Tolle TR, Gross J, Ploner M. Prefrontal gamma oscillations reflect ongoing pain intensity in chronic

back pain patients. Hum Brain Mapp. 2019;40(1):293-305. Epub 2018/09/28. doi: 10.1002/hbm.24373. PubMed PMID: 30260531; PMCID: PMC6585682.
20. Ta Dinh S, Nickel MM, Tiemann L, May ES, Heitmann H, Hohn VD, Edenharter G, Utpadel-Fischler D, Tolle TR, Sauseng P, Gross J, Ploner M. Brain dysfunction in chronic pain patients assessed by resting-state electroencephalography. Pain. 2019. Epub 2019/07/30. doi: 10.1097/j.pain.0000000000001666. PubMed PMID: 31356455.
21. Boord P, Siddall PJ, Tran Y, Herbert D, Middleton J, Craig A. Electroencephalographic slowing and reduced reactivity in neuropathic pain following spinal cord injury. Spinal Cord. 2008;46(2):118-23. Epub 2007/05/16. doi: 10.1038/sj.sc.3102077. PubMed PMID: 17502876.
22. Kisler LB, Kim JA, Hemington KS, Rogachov A, Cheng JC, Bosma RL, Osborne NR, Dunkley BT, Inman RD, Davis KD. Abnormal alpha band power in the dynamic pain connectome is a marker of chronic pain with a neuropathic component. Neuroimage Clin. 2020;26:102241. Epub 20200313. doi: 10.1016/j.nicl.2020.102241. PubMed PMID: 32203904; PMCID: PMC7090370.
23. Sarnthein J, Stern J, Aufenberg C, Rousson V, Jeanmonod D. Increased EEG power and slowed dominant frequency in patients with neurogenic pain. Brain. 2006;129(Pt 1):55-64. Epub 2005/09/27. doi: 10.1093/brain/awh631. PubMed PMID: 16183660.
24. Furman AJ, Prokhorenko M, Keaser ML, Zhang J, Chen S, Mazaheri A, Seminowicz DA. Sensorimotor Peak Alpha Frequency Is a Reliable Biomarker of Prolonged Pain Sensitivity. Cereb Cortex. 2020;30(12):6069-82. doi: 10.1093/cercor/bhaa124. PubMed PMID: 32591813; PMCID: PMC7732034.
25. Mazaheri A, Seminowicz DA, Furman AJ. Peak alpha frequency as a candidate biomarker of pain sensitivity: the importance of distinguishing slow from slowing. Neuroimage. 2022;262:119560. Epub 20220813. doi: 10.1016/j.neuroimage.2022.119560. PubMed PMID: 35973563.
26. Olesen SS, Hansen TM, Graversen C, Steimle K, Wilder-Smith OH, Drewes AM. Slowed EEG rhythmicity in patients with chronic pancreatitis: evidence of abnormal cerebral pain processing? Eur J Gastroenterol Hepatol. 2011;23(5):418-24. doi: 10.1097/MEG.0b013e3283457b09. PubMed PMID: 21399506.
27. de Vries M, Wilder-Smith OH, Jongsma ML, van den Broeke EN, Arns M, van Goor H, van Rijn CM. Altered resting state EEG in chronic pancreatitis patients: toward a marker for chronic pain. J Pain Res. 2013;6:815-24. Epub 20131125. doi: 10.2147/jpr.S50919. PubMed PMID: 24379694; PMCID: PMC3843642.
28. Hansen TM, Mark EB, Olesen SS, Gram M, Frøkjær JB, Drewes AM. Characterization of cortical source generators based on electroencephalography during tonic pain. Journal of Pain Research. 2017:1401-9.
29. Teixeira PEP, Pacheco-Barrios K, Uygur-Kucukseymen E, Machado RM, Balbuena-Pareja A, Giannoni-Luza S, Luna-Cuadros MA, Cardenas-Rojas A, Gonzalez-Mego P, Mejia-Pando PF, Wagner T, Dipietro L, Fregni F. Electroencephalography Signatures for Conditioned Pain Modulation and Pain Perception in Nonspecific Chronic Low Back Pain—An Exploratory Study. Pain Medicine. 2021;23(3):558-70. doi: 10.1093/pm/pnab293.

30. Plaghki L, Mouraux A. EEG and laser stimulation as tools for pain research. Curr Opin Investig Drugs. 2005;6(1):58-64.
31. Mussigmann T, Bardel B, Lefaucheur J-P. Resting-state electroencephalography (EEG) biomarkers of chronic neuropathic pain. A systematic review. NeuroImage. 2022;258:119351.
32. Apkarian AV, Bushnell MC, Treede R-D, Zubieta J-K. Human brain mechanisms of pain perception and regulation in health and disease. European journal of pain. 2005;9(4):463-84.
33. Drewes AM, Gratkowski M, Sami SA, Dimcevski G, Funch-Jensen P, Arendt-Nielsen L. Is the pain in chronic pancreatitis of neuropathic origin? Support from EEG studies during experimental pain. World J Gastroenterol. 2008;14(25):4020-7. doi: 10.3748/wjg.14.4020. PubMed PMID: 18609686; PMCID: PMC2725341.
34. Kenefati G, Rockholt MM, Eisert K, Zhang Q, Ok D, Gharibo CG, Voiculescu LD, Doan LV, Chen ZS, Wang J. Disruptions in Cortical Circuit Connectivity Distinguish Widespread Hyperalgesia from Localized Pain In press; Frontiers for Pain Research. 2025;6. doi: 10.3389/fpain.2025.1548500.
35. Murphy AE, Minhas D, Clauw DJ, Lee YC. Identifying and Managing Nociplastic Pain in Individuals With Rheumatic Diseases: A Narrative Review. Arthritis Care Res (Hoboken). 2023;75(10):2215-22. Epub 20230316. doi: 10.1002/acr.25104. PubMed PMID: 36785994; PMCID: PMC11210328.
36. Phillips AE, Faghih M, Kuhlmann L, Larsen IM, Drewes AM, Singh VK, Yadav D, Olesen SS, Pancreatic Quantitative Sensory Testing C. A clinically feasible method for the assessment and characterization of pain in patients with chronic pancreatitis. Pancreatology. 2020;20(1):25-34. Epub 2019/12/04. doi: 10.1016/j.pan.2019.11.007. PubMed PMID: 31787527.
37. Kurien T, Arendt-Nielsen L, Petersen KK, Graven-Nielsen T, Scammell BE. Preoperative Neuropathic Pain-like Symptoms and Central Pain Mechanisms in Knee Osteoarthritis Predicts Poor Outcome 6 Months After Total Knee Replacement Surgery. J Pain. 2018;19(11):1329-41. Epub 2018/06/20. doi: 10.1016/j.jpain.2018.05.011. PubMed PMID: 29920331.
38. Vuckovic A, Hasan MA, Fraser M, Conway BA, Nasseroleslami B, Allan DB. Dynamic oscillatory signatures of central neuropathic pain in spinal cord injury. J Pain. 2014;15(6):645-55. Epub 20140301. doi: 10.1016/j.jpain.2014.02.005. PubMed PMID: 24589821; PMCID: PMC4058526.
39. Sarnthein J, Jeanmonod D. High thalamocortical theta coherence in patients with neurogenic pain. NeuroImage. 2008;39(4):1910-7. doi: 10.1016/j.neuroimage.2007.10.019.
40. González-Roldán AM, Cifre I, Sitges C, Montoya P. Altered Dynamic of EEG Oscillations in Fibromyalgia Patients at Rest. Pain Med. 2016;17(6):1058-68. Epub 20160226. doi: 10.1093/pm/pnw023. PubMed PMID: 26921889.
41. Lee P-S, Low I, Chen Y-S, Tu C-H, Chao H-T, Hsieh J-C, Chen L-F. Encoding of menstrual pain experience with theta oscillations in women with primary dysmenorrhea. Scientific Reports. 2017;7(1):15977. doi: 10.1038/s41598-017-16039-4.

42. Fallon N, Chiu Y, Nurmikko T, Stancak A. Altered theta oscillations in resting EEG of fibromyalgia syndrome patients. Eur J Pain. 2018;22(1):49-57. Epub 20170731. doi: 10.1002/ejp.1076. PubMed PMID: 28758313; PMCID: PMC5763419.
43. Wang WE, Roy A, Misra G, Ho RLM, Ribeiro-Dasilva MC, Fillingim RB, Coombes SA. Altered neural oscillations within and between sensorimotor cortex and parietal cortex in chronic jaw pain. Neuroimage Clin. 2019;24:101964. Epub 20190731. doi: 10.1016/j.nicl.2019.101964. PubMed PMID: 31412309; PMCID: PMC6704052.
44. Petrovic P, Kalso E, Petersson KM, Ingvar M. Placebo and opioid analgesia--imaging a shared neuronal network. Science. 2002;295(5560):1737-40. Epub 20020207. doi: 10.1126/science.1067176. PubMed PMID: 11834781.
45. Kringelbach ML. The human orbitofrontal cortex: linking reward to hedonic experience. Nat Rev Neurosci. 2005;6(9):691-702. doi: 10.1038/nrn1747. PubMed PMID: 16136173.
46. Drewes AM, Bouwense SAW, Campbell CM, Ceyhan GO, Delhaye M, Demir IE, Garg PK, van Goor H, Halloran C, Isaji S, Neoptolemos JP, Olesen SS, Palermo T, Pasricha PJ, Sheel A, Shimosegawa T, Szigethy E, Whitcomb DC, Yadav D. Guidelines for the understanding and management of pain in chronic pancreatitis. Pancreatology. 2017;17(5):720-31. Epub 20170713. doi: 10.1016/j.pan.2017.07.006. PubMed PMID: 28734722.
47. Phillips AE, Afghani E, Akshintala V, Benos PY, Das R, Drewes AM, Easler J, Faghih M, Gabbert C, Halappa V, Khashab MA, Olesen SS, Saloman JL, Sholosh B, Slivka A, Wang T, Yadav D, Singh VK. Pancreatic quantitative sensory testing to predict treatment response of endoscopic therapy or surgery for painful chronic pancreatitis with pancreatic duct obstruction: study protocol for an observational clinical trial. BMJ Open. 2024;14(3):e081505.
48. Moretti DV. Theta and alpha EEG frequency interplay in subjects with mild cognitive impairment: evidence from EEG, MRI, and SPECT brain modifications. Frontiers in Aging Neuroscience. 2015;7(31); PMCID: 25926789.
49. Ebrahimzadeh E, Soltanian-Zadeh H. Editorial: Simultaneous EEG-fMRI applications in cognitive neuroscience. Frontiers in Human Neuroscience. 2024;17:1350468. doi: 10.3389/fnhum.2023.1350468; PMCID: 38239304.
50. Schneider A, Löhr JM, Singer MV. The M-ANNHEIM classification of chronic pancreatitis: introduction of a unifying classification system based on a review of previous classifications of the disease. J Gastroenterol. 2007;42(2):101-19. Epub 20070312. doi: 10.1007/s00535-006-1945-4. PubMed PMID: 17351799.
51. Sarner M, Cotton PB. Classification of pancreatitis. Gut. 1984;25(7):756-9. doi: 10.1136/gut.25.7.756. PubMed PMID: 6735257; PMCID: PMC1432589.
52. Keller S, Bann CM, Dodd SL, Schein J, Mendoza TR, Cleeland CS. Validity of the brief pain inventory for use in documenting the outcomes of patients with noncancer pain. Clin J Pain. 2004;20(5):309-18. Epub 2004/08/24. doi: 10.1097/00002508-200409000-00005. PubMed PMID: 15322437.
53. Appelhoff S, Austin HJ, Lawrence A, Li A, Mantilla Ramos YJ, O'Reilly C, Liang X, Jonte D, Mathiew S, Ole B. PyPREP: A Python implementation of the preprocessing pipeline (PREP) for EEG data. zenodo. 2023.

54. Bigdely-Shamlo N, Mullen T, Kothe C, Su K-M, Robbins KA. The PREP pipeline: standardized preprocessing for large-scale EEG analysis. Frontiers in Neuroinformatics. 2015;9(16). doi: 10.3389/fninf.2015.00016.
55. Jas M, Engemann DA, Bekhti Y, Raimondo F, Gramfort A. Autoreject: automated artifact rejection for MEG and EEG data. NeuroImage. 2017;159:417–29.
56. Larson E, Gramfort A, Engemann DA, Leppakangas J, Brodbeck C, Jas M. MNE-Python (v1.3.1). zenodo. 2023.
57. Cohen MX. Analyzing Neural Time Series Data: Theory and Practice. Cambridge, MA: MIT Press; 2014.
58. Tang X, Bi X, Qu A. Individualized Multilayer Tensor Learning with An Application in Imaging Analysis. Journal of the American Statistical Association. 2020;115(530):836–51.
59. Sun TY, Kowal DR. Ultra-efficient MCMC for Bayesian longitudinal functional data analysis. Journal of Computational and Graphical Statistics. 2025;34(1):34–46.
60. Pan SJ, Yang Q. A Survey on Transfer Learning. IEEE Transactions on Knowledge and Data Engineering. 2010;22(10):1345-59. doi: 10.1109/TKDE.2009.191.
61. Zhuang F, Qi Z, Duan K, Xi D, Zhu Y, Zhu H, Xiong H, He Q. A Comprehensive Survey on Transfer Learning. Proceedings of the IEEE. 2021;109(1):43-76. doi: 10.1109/JPROC.2020.3004555.

# Supporting Information for

## Low Frequency Oscillations in the Medial Orbitofrontal Cortex Mediate Widespread Hyperalgesia Across Pain Conditions

This file includes: Figures S1 to S3

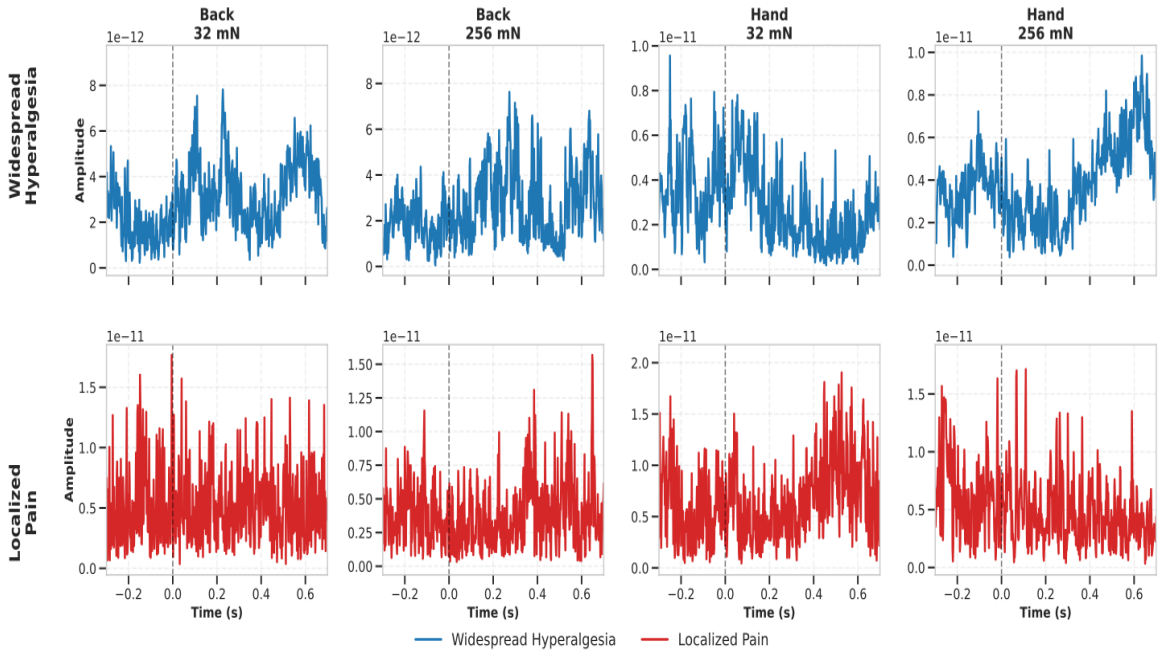


**Figure S1. Source-localized EEG traces from the left mOFC in representative cLBP participants. Top row**: Source-localized EEG traces from the mOFC (left hemisphere) for a representative participant with widespread hyperalgesia, shown across four stimulus conditions (Back 32 mN, Back 256 mN, Hand 32 mN, Hand 256 mN). **Bottom row**: Traces from a representative participant with localized pain, under the same four stimulus conditions. Epochs were extracted from -0.3 to 0.7 seconds relative to each pinprick stimulus onset. Time-frequency representations (TFRs) of power (1 to 45 Hz) were computed using real and imaginary signal components of the decomposition and transformed into decibel scale. Baseline correction was performed by subtracting the average pre-stimulus power (-0.3 to 0 s) for each trial per frequency. Corrected dB power responses were then averaged across trials per condition to yield subject- and stimulus condition-specific TFRs for each of the four regions of interest (bilateral mOFC and dlPFC).

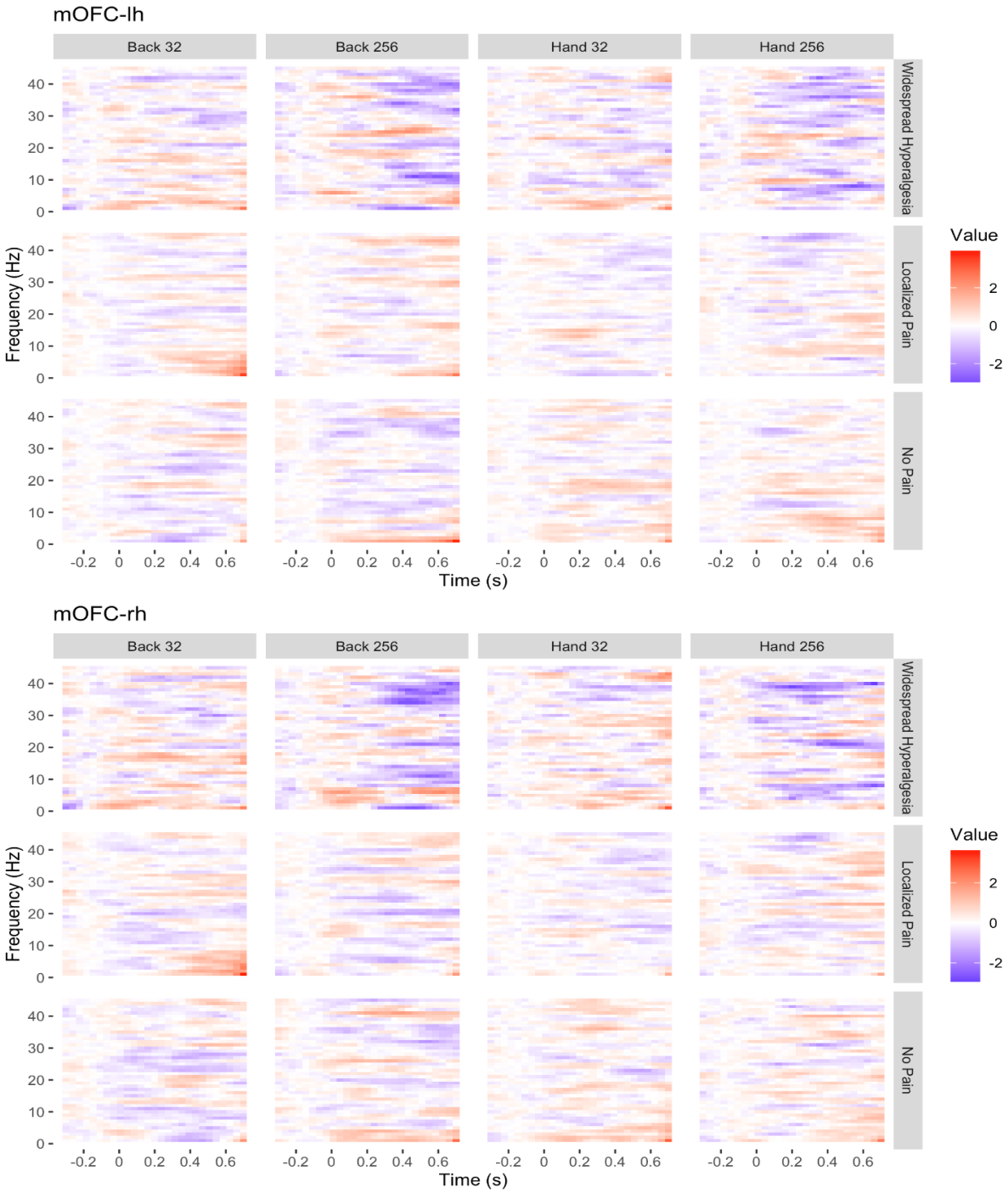


**Figure S2. Time-frequency EEG responses in the mOFC by stimulus condition and pain phenotype in the chronic low back pain (cLBP) cohort (n = 67)**. Group- and stimulus-specific averaged time-frequency representations (TFRs) for the cLBP cohort, averaged across participants within each pain phenotype group (Widespread Hyperalgesia, Localized Pain, No Pain). Top panels show responses from the left mOFC; bottom panels from the right mOFC. Each panel displays baseline-corrected decibel power from -0.3 to 0.7 seconds post-stimulus across four conditions: Back 32 mN, Back 512 mN, Hand 32 mN, and Hand 512 mN.

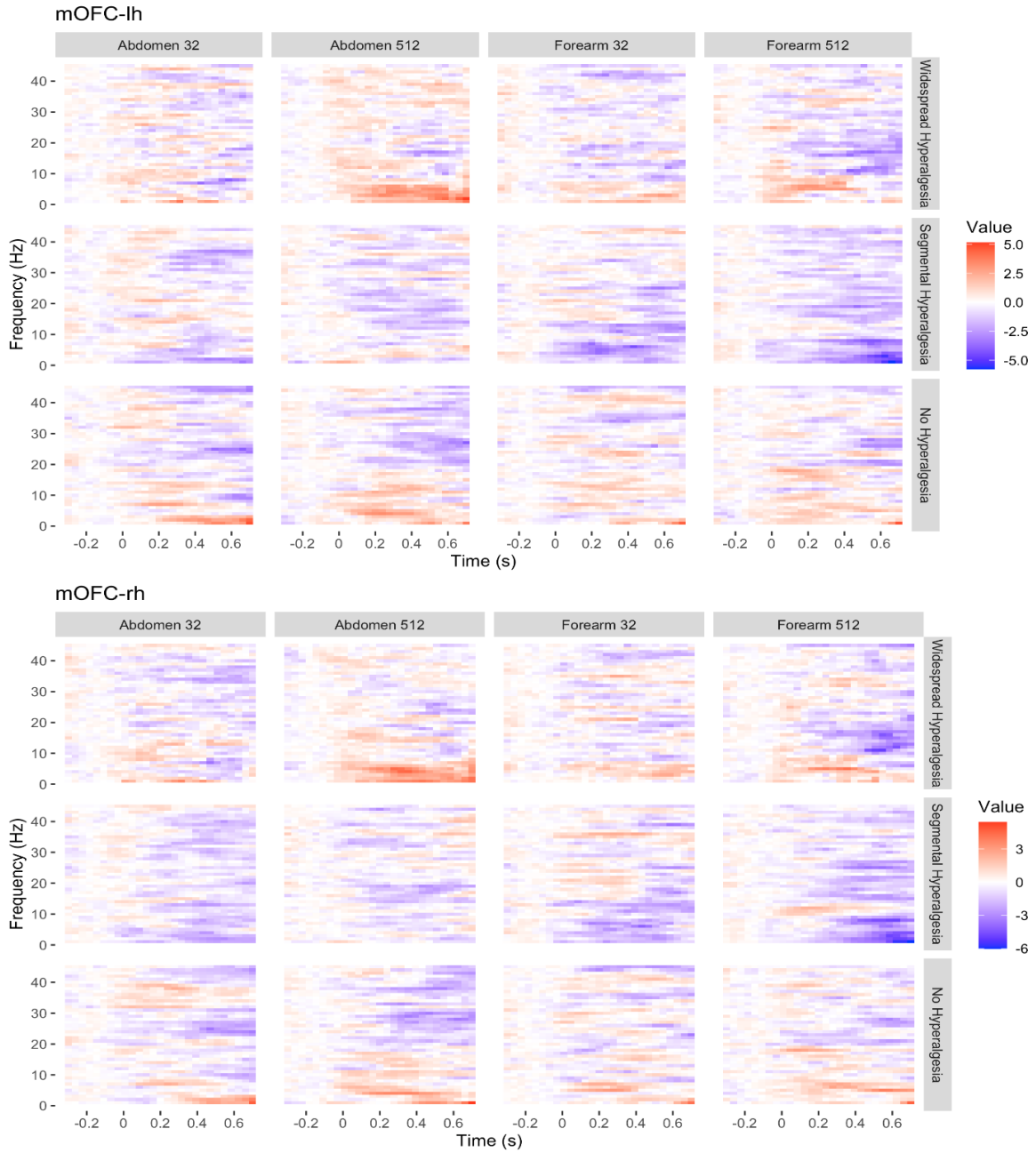


**Figure S3. Time-frequency EEG oscillatory responses in the mOFC by stimulus condition and pain phenotype in the chronic pancreatitis (CP) cohort (n = 18)**. Group-averaged time-frequency representations (TFRs) are shown for each pain phenotype group (Widespread, Segmental, No Hyperalgesia), stratified by stimulation site and intensity: Abdomen 32 mN, Abdomen 512 mN, Forearm 32 mN, and Forearm 512 mN. Each panel displays baseline-corrected power (in decibels) from –0.3 to 0.7 seconds post-stimulus. Top panels reflect responses from the left mOFC; bottom panels from the right mOFC. The widespread hyperalgesia group (top row) exhibited elevated delta/theta (1–7 Hz) power under high-intensity stimulation at the affected site (Abdomen 512 mN), compared to the segmental hyperalgesia group (middle row). The segmental hyperalgesia group showed relatively reduced delta/theta activity at the unaffected site (Forearm 512 mN), suggesting differential neural processing of noxious input across phenotypes.